JOURNAL OF SOLID STATE CHEMISTRY 36, 74–80 (1981)

Electron Microscope Observation of Lattice Defects in the Fe–Cr σ-Phase

TSUTOMU ISHIMASA, YASUYUKI KITANO, AND YUKITOMO KOMURA[1]

Department of Materials Science, Faculty of Science, Hiroshima University, Higashi-senda-machi, Naka-ku, Hiroshima 730, Japan

Received February 11, 1980; in revised form April 21, 1980

The lattice image of the Fe–Cr σ-phase was observed by high-resolution electron microscopy with the c axis of the tetragonal cell parallel to the incident beam. It was found that bright dots of the observed image correspond to the positions of atoms in the $z = \pm 1/4$ planes of the σ-phase structure. Sequence faults were found in the irregular part of the lattice image. The analysis of the faults shows that an extra plane of $1/2\, a_0$ width is inserted into the regular structure and one side of the fault is slightly shifted parallel to the fault plane with respect to the other side, which is consistent with the model proposed by Frank and Kasper. A unit cell step of the sequence faults was found and a model of the step was proposed.

Introduction

The Fe–Cr σ-phase is stable at about equicomposition and at temperatures below about 815°C (*1*). The crystal structure of the σ-phase has been investigated by Bergman and Shoemaker (*2*) by means of X-ray diffraction. The structure is tetragonal, space group $D_{4h}^{14} - P4_2/mnm$ with lattice constants $a_0 = 8.800$ Å and $c_0 = 4.544$ Å for the Fe-46.5 at% Cr σ-phase. The structure of the σ-phase is understood as topologically close-packed structure from the point of view of the geometrical construction (*3–5*).

The possibility of the existence of sequence faults, which are typical planar defects in the σ-phase structure, was first predicted by Frank and Kasper (*3*). Marcinkowski and Miller proved the existence of the sequence faults in the Fe–Cr σ-phase by means of electron microscopy (*6*). They have shown that the contrast of the sequence faults in dark field images is explained by the model proposed by Frank and Kasper. Stenberg and Andersson have taken two-dimensional lattice images of regular crystals of the Fe–Mo and Cr–Fe–Ni σ-phase by a high-resolution electron microscope (*7–9*).

The purpose of the present investigation is to observe the lattice image of the Fe–Cr σ-phase by using a high-resolution electron microscope in order to find characteristic lattice defects through the irregularity of the image. Further, the type and structure of the lattice defects are studied more directly and precisely.

[1] All correspondence should be sent to Y. Komura.

022-4596/81/010074-07$02.00/0

The Structure of the σ-Phase and the Model of the Sequence Fault

The projection of the σ-phase structure onto the c plane is given in Fig. 1. The structure is regarded as a stacking of $z = 0$, 1/4, 1/2, and $-1/4$ atomic planes. The pattern of triangles and hexagons observed at $z = 0$ and $z = 1/2$ is known as kagomé tiling. The plane at $z = 1/2$ is related by rotation of $\pi/2$ to the plane at $z = 0$ after shifting by [1/2, 1/2, 0]. The positions of atoms in the $z = 1/4$ plane are the same as those in the $z = 1/4$ plane. These atoms are located halfway between main layers at $z = 0$ and 1/2, centering the hexagonal antiprisms. In the regular structure, lines connecting the atoms at $z = 1/4$ or $-1/4$ form a row indicated by arrows shown in Fig. 1. It is characteristic that "+" and "−" are repeated alternately in the regular structure, where "+" means the upward arrow of which the y component is positive and "−" means the downward arrow of which the y component is negative.

An example of a model of the sequence fault lying in the (100) plane proposed by Frank and Kasper (*3*) and Marcinkowski and Miller (*6*) is given in Fig. 2. In this model the distortion of the structure due to the sequence fault is relaxed so as to reduce the shear strain in the vicinity of the fault. At this sequence fault, an extra plane of 1/2

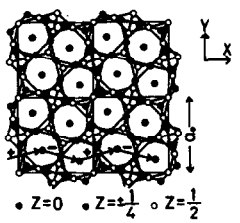

FIG. 1. The projection of the σ-phase structure onto the c plane. A fine line square ($a_0 \times a_0$) shows a unit cell of the σ-phase. Arrows in the figure connect the atoms in the $z = 1/4$ or $-1/4$ plane. When a sequence fault lying in the (100) plane is considered, it is useful to connect the arrows in the x direction. "+" and "−" mean the upward and downward arrows, respectively.

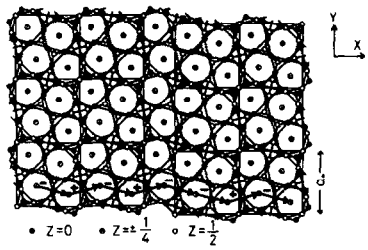

FIG. 2. A model of the sequence fault "Type −2." In this model the right part of the crystal is displaced by [1/2, $\bar{2}$/15,0] which corresponds to [4.40, $\overline{1.17}$, 0] Å.

a_0 width is inserted into the regular structure and the right part of the crystal is shifted by 2/15 a_0 in the $\bar{y}$ direction. In other words, "−" repeats two times in succession at this sequence fault, so let us call this fault "Type −2" for convenience. Similarly a sequence fault at which "+" repeats two times, "+" repeats three times, or "−" repeats three times is considered. We call them "Type +2," "Type +3," and "Type −3," respectively. Here "Type +N" is the reverse of "Type −N," where N means an integer.

Experiments

Alloy specimens of Fe–Cr were offered by Professor K. Kumada of Ehime University. The alloys were prepared by melting pure Fe, Cr, and Ni together in an induction furnace and forged, then annealed at 1000°C for 2 hr. The particular alloy examined in this study was analyzed chemically as 44.90 at% Cr, 2.20 at% Ni, 0.86 at% Si, 0.35 at% N, 0.34 at% C, 0.22 at% Mn, 0.072 at% Al, and Fe balance. Kumada and Naohara reported that the formation of the σ-phase is promoted by an addition of a small amount of Ni (*10*). It seems that the cracks formed after the transformation from α- to σ-phase are decreased by this addition. The specimen was transformed to the σ-phase completely by an annealing at 750°C for 7 hr. Thin slices about 0.3 mm

thick were prepared by using a diamond cutter. A solution of 133 ml glacial acetic acid, 25 g chromium trioxide, and 7 ml distilled water was used for electrolytic polishing. This polishing was done using stainless-steel cathodes at a potential of 19 ~ 25 V dc. Preliminary observations have been done under a JEM 200A electron microscope in Hiroshima University. High-resolution studies were performed with a Hitachi H700 electron microscope in Naka works of Hitachi Ltd., equipped with a double tilting stage of top entry (HK6) and operating at 200 kV. The specimen was oriented so that the c axis of the tetragonal cell was parallel to the incident beam. The electron diffraction pattern thus obtained shows the $hk0$ reciprocal net. In this orientation the lattice images were recorded at a magnification of 30,4000 after inserting an objective aperture centered at 000 which included all the reflections inside the 400 reflection.

Results

An example of the lattice images thus observed is given in Fig. 3. A repeating unit of the image coincides with the c-projection

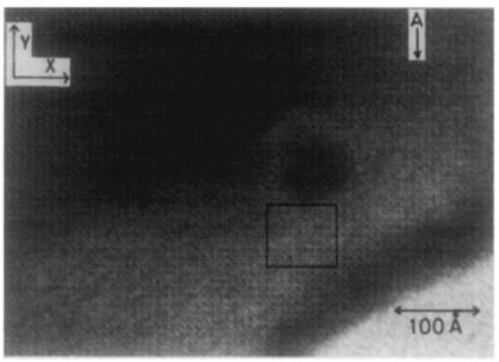

FIG. 3. A lattice image of the Fe–Cr σ-phase. A detail inside the unit cell is observed at the second equal thickness contour. At the thicker part of the crystal the bright dots of the lattice image extend to the [1$\bar{1}$0] direction. A sequence fault is observed at "A."

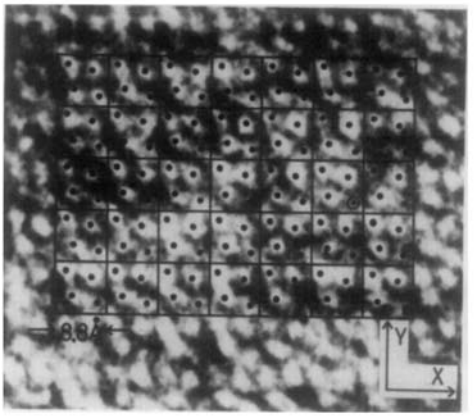

FIG. 4. The magnified image of the enclosed part of the rectangle in Fig. 3. The unit cells of the σ-phase and the positions of the atoms in the $z = \pm 1/4$ planes are indicated as squares and black dots, respectively. One of the four bright dots forming the diamond in the unit cell is often observed relatively weak. An example of these dots is indicated by ⊙.

of the unit cell (8.8 × 8.8 Å) of the σ-phase structure. A detail inside the unit cell was observed at the second equal thickness contour. The part enclosed with a rectangle in Fig. 3 is magnified in Fig. 4. The unit cells of the σ-phase and the atoms in the $z = \pm 1/4$ planes are illustrated as squares and black dots, respectively, in Fig. 4. It can be recognized that the bright dots of the image correspond with the positions of the atoms in the $z = \pm 1/4$ planes of Fig. 1.

The calculation of the lattice image has been done, based on the dynamical theory of electron diffraction (*11*) under the conditions of 200 kV accelerating voltage and beam incidence along the c axis. The partial ordering scheme in this alloy was assumed after Algie and Hall (*12*) for the calculation of the structure factor. The dynamical calculation was carried out for 81 reflections inside 440. The aperture was set to allow 25 beams inside 220 to contribute to the images. The spherical aberration coefficient was assumed as 3 mm. The calculation was carried out from 1200 Å overfocus to 1800

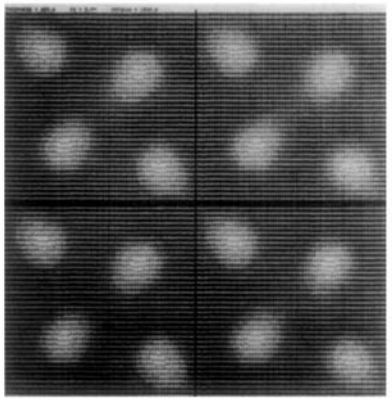

FIG. 5. A calculated image of the Fe–Cr σ-phase.

Å underfocus at the crystal with the thickness of less than 250 Å. An example of the calculated image is given in Fig. 5 with 1200 Å underfocus for the crystal with the thickness of 225 Å. This calculated image shows a good agreement with the experimentally obtained image (Fig. 4). So it is concluded that the positions of the bright dots in Fig. 4 correspond with those of the atoms in the $z = \pm 1/4$ planes. However, one of the four bright dots forming the diamond in the unit cell was often observed relatively weak in Fig. 4. Further, at the thicker part of the crystal the bright dots of the lattice image extend to the $[1\bar{1}0]$ direction in Fig. 3. It is considered that the incident beam inclined slightly from the c axis to the [110] or $[\bar{1}\bar{1}0]$ direction in our experiment. As a result of the calculation under the various conditions of defocus and thickness, it is seen that the contrast of the image is low for the thin crystal with the thickness of less than 100 Å. For the thicker crystal with thickness 100 ~ 250 Å, other positions sometimes become brighter besides the positions of the atoms in the $z = \pm 1/4$ planes under the underfocus condition. When the image is calculated under the conditions as given in Table I, only the atom positions at $z = \pm 1/4$ become bright and the contrast of the image is higher and consequently images like Fig. 5 are obtained. This image (Fig. 5) resembles the lattice image of the Cr–Fe–Ni σ-phase given by Stenberg (*8, 9*).

TABLE I

CONDITIONS FOR TAKING THE LATTICE IMAGE LIKE FIG. 5

Under focus (Å)	Thickness (Å)
1000	250
1200	200 ~ 250
1400	100 ~ 225
1600	125 ~ 200
1800	125 ~ 175

At column "A" in Fig. 3 a fault lying in the (100) plane is observed which is accompanied by irregularity of the lattice image. The magnified part including the fault "A" is given in Fig. 6. The unit cells of the σ-phase and the atoms in the $z = \pm 1/4$ planes are illustrated in Fig. 6 in a similar manner to Fig. 4. From Fig. 6 it can be seen that an extra plane of $1/2\, a_0$ width is inserted into the regular structure and the right part of the crystal is slightly shifted in the $\bar{y}$ direction at the fault "A." In other words, "–" repeats two times in succession at the fault "A." In order to know the displacement at the fault precisely, the coordinates of the bright dots were measured at both sides of

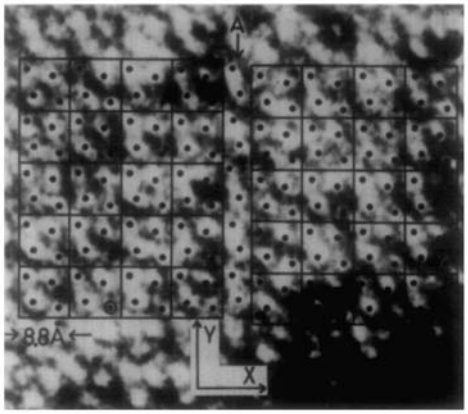

FIG. 6. The magnified image of the sequence fault in Fig. 3. An extra plane of 4.7 Å width is inserted into the regular structure and the right part of the crystal is shifted by 1.3 Å from the left one in the $\bar{y}$ direction.

the crystal under an optical microscope and the displacement was estimated with the aid of the least squares method. The displacement thus obtained is [4.7, $\overline{1.3}$, 0] Å, and the value coincides with the estimated displacement of [4.40, $\overline{1.17}$, 0] Å, which corresponds to [1/2, $\bar{2}$/15, 0], at the sequence fault "Type −2" within the experimental error.

A lattice image including a unit cell step "B" of the sequence faults is shown in Fig. 7. "C" and "D" indicate the columns of the sequence faults. The sequence fault "D" steps out in the x direction by an amount of a_0 (8.8 Å) at "B," and then changes to the sequence fault "C." This image was observed at the fourth equal thickness contour. Only the unit cell ($a_0 \times a_0$) was resolved in the image presumably because of the thickness and a slight inclination of the specimen. The displacement at each sequence fault was estimated from the shift of the unit cell in the lattice image.

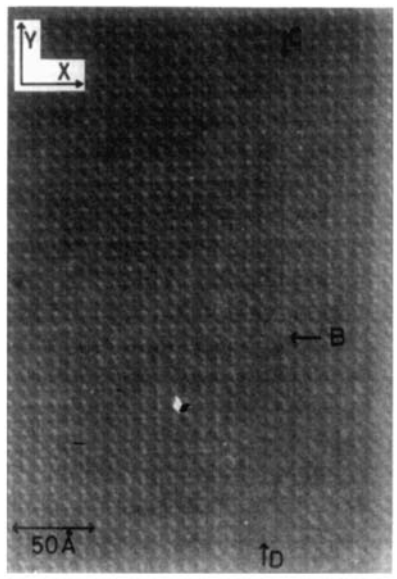

FIG. 7. A lattice image including a unit cell step of the sequence faults. The "C" and "D" indicate the sequence faults. The sequence fault "D" steps out in the x direction by the amount of a_0 at "B" and changes to the sequence fault "C."

The structure of these sequence faults thus determined are "Type −2" at the both sides of the step. So the type of the sequence faults does not change at the step.

Discussion

The two-dimensional lattice image of the Fe–Cr σ-phase could be observed under the condition where the c axis of the tetragonal cell was parallel to the incident beam. The calculated lattice image based on the dynamical theory of electron diffraction was compared with the observed one. It was found that the bright dots of the lattice image correspond to the positions of the atoms in the $z = \pm 1/4$ planes. Sequence faults were found in the lattice image and the structure of the faults was analyzed directly from the lattice image by using the model proposed by Frank and Kasper.

Marcinkowski and Miller classified the sequence faults into six types (*6*). The sequence faults "f_1^+" and "f_2^-" in their classification correspond to "Type −2" in the present paper, because the structure of "f_1^+" is identical with that of "f_2^-" unless the mechanism of the formation of the sequence faults is considered. Similarly "f_1^-" and "f_2^+" correspond to "Type +2." "f_3^+" and "f_3^-" correspond to "Type +3" and "Type −3," respectively. As mentioned in the previous section, "Type $-N$" is the reverse of "Type $+N$." So it is essential to know how many times the arrows of "+" or "−" repeat in succession at the sequence fault. A sequence fault is considered to be accompanied by a strain around it in general. Marcinkowski and Miller discussed that this strain is due to the difference in the displacement between the $z = 0$ and $z = 1/2$ planes at the sequence fault and sequence faults of "Type $\pm N$ ($N \geq 3$)" would be unstable because of their higher energy. In our observations only "Type ±2" were observed. This fact is consistent with their consideration.

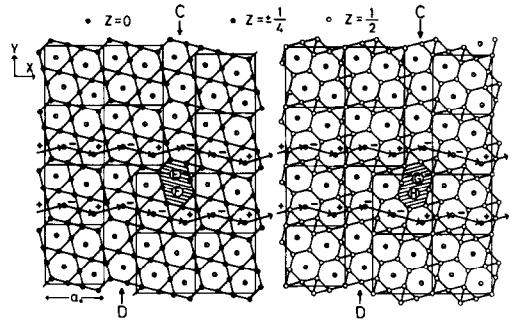

FIG. 8. A model of the unit cell step of the sequence faults. The "C" and "D" correspond to those in Fig. 7. The atom positions of "E," "F," "G," and "H" are in the $z = \pm 1/4$ planes, but some of these positions are assumed to be vacant.

Marcinkowski and Miller observed steps of the sequence faults in low magnified images (*6*). The unit cell step observed at "B" in Fig. 7 can be considered as one of the steps with the shortest interval between the two sequence faults. A model of this step is deduced from the observed fact that the sequence faults are "Type −2" at both sides of this step. The model thus obtained is given in Fig. 8. The $z = 0$ and $z = 1/2$ planes are given separately for convenience. In Fig. 8 the faults "C" and "D" correspond to those in Fig. 7, respectively. The $z = 0$ and $z = 1/2$ planes of this model can be constructed of triangles and hexagons. But the structure in the shaded portions in Fig. 8 is in question, namely, the atomic distances from "E" to "F" and from "G" to "H" are abnormally short. Therefore, it is assumed that some of these atoms are properly taken off in real structure so that the abnormal condensation does not occur.

The calculated image in our paper (Fig. 5) is geometrically different from that of the Fe–Mo σ-phase given by Stenberg and Andersson (Fig. 5 in Ref. *7*). The crystal thickness 225 Å is used in our calculation, while 30 Å was used in their calculation. In the present case the crystal thickness of 225 Å is considered resonable for the following reasons. The second equal thickness contour is predicted to appear at the thickness of about 250 Å by the dynamical calculation and actually the lattice image is obtained near the contour. The contrast of the calculated image with the crystal thickness of 30 Å is quite low in our calculation.

Intersections of the sequence faults lying in the (100) and (010) planes, which were observed frequently by Marcinkowski and Miller, were also observed in the present specimen. The atomic configuration at the intersection may be elucidated through the observation of the lattice image.

Acknowledgments

The present authors wish to thank Prof. K. Kumada of Ehime University for preparation and offering of the alloy specimens and Mr. S. Okamura and Mr. T. Tsuruta of Naka works of Hitachi Ltd. for taking the lattice images. All the calculations were carried out on a HITAC 8700 computer at the Computing Center of Hiroshima University. They are grateful to Prof. F. E. Fujita of Osaka University for continuous encouragement during the course of this study. The present work has been supported partly by a Scientific Research Grant from the Ministry of Education, to which the authors' thanks are due.

References

1. M. HANSEN, "Constitution of Binary Alloys," 2nd ed., p. 525. McGraw–Hill, New York (1958).
2. G. BERGMAN AND D. P. SHOEMAKER, *Acta Crystallogr.* **7**, 857 (1954).
3. F. C. FRANK AND J. S. KASPER, *Acta Crystallogr.* **12**, 483 (1959).
4. C. G. WILSON AND F. J. SPOONER, *Acta Crystallogr. A* **29**, 342 (1973).
5. A. K. SINHA, "Progress in Materials Science, Vol. 15, Topologically Close-Packed Structures of Transition Metal Alloys." Pergamon Press, Oxford (1973).
6. M. J. MARCINKOWSKI AND D. S. MILLER, *Phil. Mag.* **7**, 1025 (1962).
7. L. STENBERG AND S. ANDERSSON, *J. Solid State Chem.* **28**, 269 (1979).
8. L. STENBERG, AIP Conference Proceedings 53, Hawaii, 259 (1979).
9. L. STENBERG, *Chem. Scripta,* in press.

10. K. KUMADA AND T. NAOHARA, *Memoirs Ehime Univ.* Sect. 3 (Engineering), **8,** 3, 123 (1976).
11. P. B. HIRSCH, A. HOWIE, R. B. NICHOLSON, D. W. PASHLEY, AND M. J. WHELAN, "Electron Microscopy of Thin Crystals," Chap. 12. Butterworths, London (1965).
12. S. H. ALGIE AND E. O. HALL, *Acta Crystallogr.* **20,** 142 (1966).